

# Optical Characterization of Laser-Synthesized Anatase TiO<sub>2</sub> Nanopowders by Spectroscopic Ellipsometry and Photoluminescence Measurements\*

M. ŠĆEPANOVIĆ<sup>†</sup>, M. GRUJIĆ-BROJČIN, M. MIRIĆ, Z. DOHČEVIĆ-MITROVIĆ  
AND Z.V. POPOVIĆ

Center for Solid State Physics and New Materials, Institute of Physics, Belgrade, Serbia

Nanosized titania (TiO<sub>2</sub>) is synthesized by laser-induced pyrolysis using TiCl<sub>4</sub> as a liquid precursor. X-ray diffraction and Raman scattering confirmed anatase structure of TiO<sub>2</sub> nanocrystals. The dielectric function  $\varepsilon(\omega)$  of TiO<sub>2</sub> nanopowders has been determined by spectroscopic ellipsometry in the energy range from 1.5 to 6 eV at room temperature. The features observed in  $\varepsilon(\omega)$  have been fitted to analytical line shapes by using the second derivatives of experimental spectra. The energies corresponding to different interband electronic transitions have been determined. Photoluminescence measurements have been carried out in vacuum for  $T = 20$  K and  $T = 300$  K. Under laser irradiation with sub-band gap photon energy, anatase nanocrystals have displayed strong visible photoluminescence emission. In this broad photoluminescence band different variations of line shape and position with excitation energy and temperature are observed for nanopowders with different crystallite size, pointing out to the various electronic transitions mediated by defect levels within the band gap.

PACS numbers: 81.07.Wx, 78.67.Bf, 73.22.-f, 07.60.Fs, 78.55.-m

## 1. Introduction

Anatase TiO<sub>2</sub> have attracted a lot of attention as wide-band gap semiconductor nanomaterial with numerous applications, including photocatalysis, optical coating, and photoelectrochemical solar cells [1]. Accurate knowledge of anatase dielectric function is a source of valuable experimental information about its electronic band structure, indispensable for the design and analysis of various optoelectronic devices. Spectroscopic ellipsometry (SE) is rapidly developing technique, recognized as powerful non-destructive and contactless method for characterization of solids. Namely, SE is a very sensitive measurement technique for investigating optical response of solids, especially semiconductors, and determining their complex dielectric function [2, 3]. Among variety of reports on optical constants of TiO<sub>2</sub>, only few are available on the optical characterization of TiO<sub>2</sub> nanopowders using SE [4]. In the present work, anatase TiO<sub>2</sub> nanopowders are characterized by SE in conjunction with photoluminescence (PL) spectroscopy.

## 2. Experimental methods

Titanium dioxide nanopowders were synthesized by laser-induced pyrolyses using TiCl<sub>4</sub> as a liquid precursor [5]. The produced powders were calcined in air for 4 h at 500°C. Specific surface area of as-produced nanopowders was measured by Brunauer–Emmett–Teller (BET) method and for the samples, labeled as TiS12 and TiS57, was 84 and 110 m<sup>2</sup>/g, respectively. Corresponding X-ray diffraction (XRD) patterns showed characteristic diffraction peaks for the anatase phase present in both samples. The average crystallite size, roughly estimated from the main XRD peak (around  $2\theta = 25.3^\circ$ ) by the Sherrer formula, was 18 and 13.7 nm for TiS12 and TiS57, respectively. Raman measurements also confirmed that both investigated TiO<sub>2</sub> nanocrystals had an anatase structure [6].

The ellipsometric spectra of the TiO<sub>2</sub> nanopowders were measured using SOPRA GES-5 variable angle ellipsometer in rotating polarizer configuration. The SE data ( $\cos(\Delta)$ ,  $\tan(\Psi)$ ) were collected at room temperature, in the range from 1.5 to 6.0 eV with resolution of 0.05 eV, for three incidence angles of 60, 65 and 70° to ensure a consistent and accurate determination of the dielectric constant of the material. Bulk calculations were used to analyze the ellipsometric spectra and determine the dielectric functions of anatase nanopowders from measured SE data.

Photoluminescence spectra excited by two lines of Ar<sup>+</sup> ion laser with photon energy 2.41 and 2.71 eV were collected by using Jobin-Yvon U1000 monochromator and photomultiplier as detector. Laser beam power at the sample surface was about 0.05 W/cm<sup>2</sup>.

\* Revised paper, corrigenda November 19, 2011. Fig. 3 and last paragraph of Section 4 are changed and Refs. 21 and 22 are added.

<sup>†</sup> corresponding author; e-mail: [maja@phy.bg.ac.rs](mailto:maja@phy.bg.ac.rs)

### 3. Results of spectroscopic ellipsometry

A model, based on effective medium approximation (EMA) of a dielectric function of nanopowder, described as a mixture of bulk polycrystalline material and voids, is often used to interpret the experimental results. Generally, EMA may be used if material is composed of phases with the size much smaller than the radiation wavelength, but large enough to retain its bulk properties [7]. If component sizes decrease, it may not be possible to describe the components using bulk reference data due to size effects or strain [7]. Namely, it appears that this approach in UV and visible range does not produce good results in modelling experimental dielectric function of anatase nanopowders, although very good agreement was previously obtained in far-infrared region [8]. Therefore more proper model of the dielectric function of anatase nanopowder is applied in this study by using critical point (CP) analysis [9, 10]. This model has been successfully applied to identify and evaluate the energy of the electronic transitions in different semiconducting materials [10, 11].

There is general agreement that the absorption edge of bulk anatase crystal around 3.2 eV is associated with indirect optical band gap transitions (Ref. [12] and references therein). It is also known that widening of band gap might be expected in nanosized materials [13]. Indeed, it is shown that decreasing the diameter of spherical nanoparticles in anatase  $\text{TiO}_2$  by 10 nm is accompanied by the band-gap increase for the value of  $\Delta E_g \approx 0.2$  eV [14] or  $\Delta E_g \approx 0.4$  eV [15]. Beside the indirect band-gap transition mentioned above, the transition at about 3.8 eV has been ascribed to the direct optical band gap in different anatase  $\text{TiO}_2$  films [16, 17]. Few direct interband transitions with the energy higher than 3.8 eV are also predicted [18, 19] and experimentally registered [16, 20] in anatase  $\text{TiO}_2$ . Also, in case of  $\text{TiO}_2$  amorphous films, measured pseudodielectric function spectra have shown three distinct structures at about 3.3, 3.9 and 4.9 eV, which have been assigned to the transitions at the  $E_1$ ,  $E_1 + \Delta E_x$  and  $E_2$  CPs in the Brillouin zone, respectively [4].

The spectra of the real  $\varepsilon_1(\omega)$  and imaginary  $\varepsilon_2(\omega)$  part of the complex dielectric function  $\varepsilon(\omega)$  of TiS12 and TiS57 samples obtained by bulk calculation from SE experimental data are shown in Fig. 1a and b, respectively. The features observed in range from 3 to 5 eV of the  $\varepsilon(\omega)$  spectra are ascribed to interband CPs, which are related to regions of the band structure with large or singular point electronic density of states [9]. Those structures are analyzed by standard analytic line shapes [10]:

$$\varepsilon(\omega) = C - A \exp(i\varphi)(\omega - E + i\gamma)^m, \quad (1)$$

where a CP is described by the amplitude  $A$ , threshold energy  $E$ , broadening  $\gamma$  and phase angle  $\varphi$ . The exponent  $m$  takes the values of  $-1/2$  and  $1/2$  for one- (1D) and three-dimensional (3D) CPs, respectively. Two-dimensional (2D) CPs are described with  $m = 0$  and corresponding analytical line shape is given by  $\varepsilon(\omega) =$

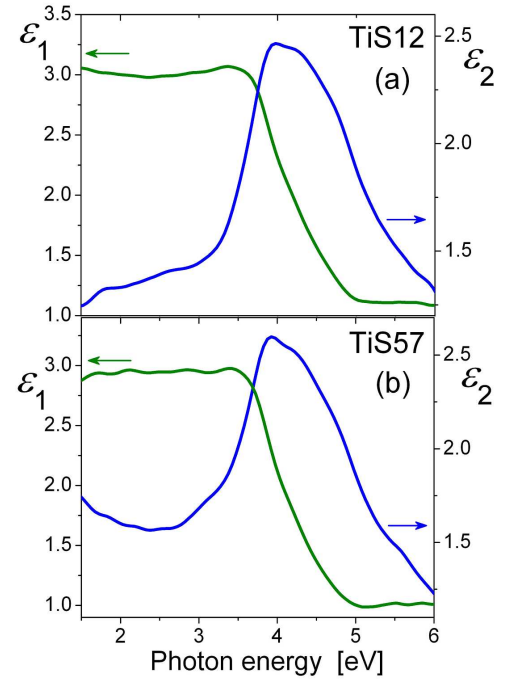


Fig. 1. Real ( $\varepsilon_1$ ) and imaginary ( $\varepsilon_2$ ) part of the dielectric function vs. energy for (a) TiS12 and (b) TiS57 anatase nanopowders.

$C - A \exp(i\varphi) \ln(\omega - E + i\gamma)$ . Discrete excitons with a Lorentzian line shape (0D) are represented by  $m = -1$ .

The 2nd derivative spectra of the complex dielectric function  $d^2\varepsilon(\omega)/d\omega^2$  were calculated by standard technique of smoothing polynomials to obtain the CP parameters [9]. It is given in analytic form as follows [11]:

$$\frac{d^2\varepsilon}{d\omega^2} = A' \Omega^{(m-2)/2} \times \left( \cos((m-2) \arccos((\omega - E)/\Omega^{1/2}) + \varphi) + i \sin((m-2) \arccos((\omega - E)/\Omega^{1/2}) + \varphi) \right), \quad (2)$$

with  $\Omega = (\omega - E)^2 + \gamma^2$ . Let us note that for  $\omega \neq 0$ ,  $A' = -m(m-1)A$ , but for  $m = 0$ ,  $A'$  must be equal to  $A$ . The parameters  $A$ ,  $E$ ,  $\gamma$  and  $\varphi$  can be calculated by fitting the numerically obtained second derivative spectra of the experimental  $\varepsilon(\omega)$  to Eq. (2).

Figure 2 shows the experimental spectra of the 2nd derivatives of the experimental dielectric functions  $\varepsilon_1(\omega)$  and  $\varepsilon_2(\omega)$  for TiS12 and TiS57 anatase nanopowders. The fitting curves, obtained by taking into account the electronic transitions in the range from 3 to 5 eV, according to Eq. (2), are also shown. The fitting procedure considers the CPs of 3D type with values  $m = 1/2$ ,  $A > 0$ , and  $\varphi > 0$  in the  $E_1$  region (around 3.5 eV), whereas the CPs of 1D type with values  $m = -1/2$ ,  $A > 0$ , and  $\varphi > 0$  are assumed in the  $E_2$  region (above 4 eV). The fitting parameters  $E$  and  $\gamma$  of the CPs for the studied anatase nanopowders are listed in Table. These results point out that the energy of  $E_1$  CP, which can be related to indi-

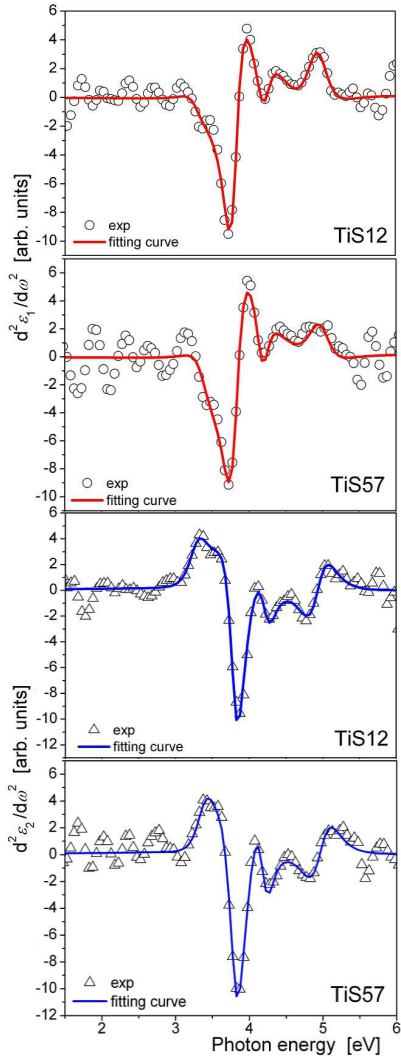


Fig. 2. 2nd derivatives of real,  $\varepsilon_1(\omega)$ , and imaginary,  $\varepsilon_2(\omega)$ , components of dielectric functions obtained by SE measurements of TiS12 and TiS57 anatase nanopowders, together with the fitting curves determined by Eq. (2).

rect energy band gap transition, is higher in nanopowder with smaller crystallite size. Namely, this energy reaches 3.384 eV in TiS57, whereas in TiS12 its value is 3.285 eV. Such increase ( $\approx 0.1$  eV with crystallite size decrease by  $\approx 5$  nm) coincides with the behavior predicted for the energy band gap in anatase nanostructures [14, 15].

However, the energy of  $E_1 + \Delta E_1$  CP, related to the direct electron transitions between valence and conduction bands, which probably corresponds to direct optical band gap, has similar value ( $\approx 3.81$  eV) in both nanopowders. Two more features denoted by  $B$  and  $E_2$  in Table, at  $\approx 4.2$  and  $\approx 4.9$  eV respectively, can also be ascribed to direct interband electron transitions previously registered in anatase thin films [16, 20]. Finally, note that some low intensity peaks in the subband gap energy region ( $< 3$  eV) are observed, but corresponding electron

TABLE  
Fit parameters of the CPs for the studied anatase nanopowders.

Transitions	$E$ [eV]	$\gamma$ [eV]
Sample TiS12		
$E_1$	3.285	0.210
$E_1 + \Delta E_1$	3.810	0.150
$B$	4.211	0.202
$E_2$	4.931	0.301
Sample TiS57		
$E_1$	3.384	0.215
$E_1 + \Delta E_1$	3.815	0.167
$B$	4.135	0.179
$E_2$	4.969	0.310

transitions are not included in this analysis, mostly because of the difficulties in precise evaluation of their energies in the 2nd derivative spectra. To analyze these features, additional SE measurements with higher resolution are necessary, and this will be the subject of further research.

#### 4. PL results

Under the laser irradiation with subband photon energy of 2.41 and 2.71 eV anatase nanocrystals displayed strong visible light emission, even at excitation power as low as 0.05 W/cm<sup>2</sup>. The line shape and position of this broad luminescence band vary with excitation energy and temperature, as can be seen from Fig. 3.

The analysis of those variations suggests that the PL spectra of nanopowder TiS12, with larger crystallite size, are dominated by a radiative recombination of electrons via intrinsic surface states for all applied excitation energies and temperatures. The energy of these optical electron transitions is about 2.2 eV [1, 6]. However, excitation of the sample with smaller nanocrystallites, TiS57, by higher photon energies (close enough to the energy band gap) activates self-trapped exciton luminescence with the energy of  $\approx 2.41$  eV [4] (and the references therein). PL blueshift with sample cooling also points out to the recombination of self-trapped excitons as dominant PL mechanism in TiS57 nanopowder.

However, excitation of the sample with smaller nanocrystallites, TiS57, by higher photon energies (2.71 eV, close enough to the energy bandgap) activates self-trapped exciton luminescence [1, 6]. With temperature decrease, the PL intensity in the sample TiS57 increases and the band maximum position is redshifted from  $\approx 2.30$  eV at room temperature to  $\approx 2.24$  eV at 20 K (Fig. 3b). Such behavior points out to the recombination of self-trapped excitons as dominant PL mechanism in this nanopowder [21, 22].

#### 5. Conclusion

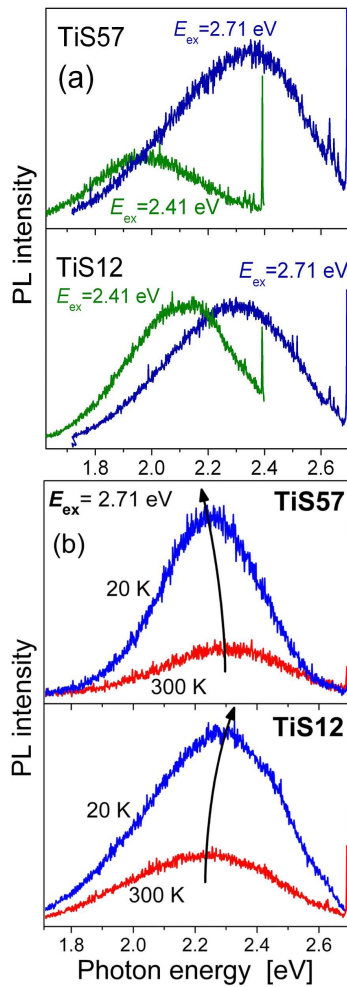


Fig. 3. PL spectra of anatase nanopowders with variation of laser excitation energy (a) and temperature (b).

Spectroscopic ellipsometry has been used to determine room temperature pseudodielectric function spectra of laser synthesized anatase  $\text{TiO}_2$  nanopowders. The measured  $\varepsilon(\omega)$  spectra revealed structures around indirect band gap and higher energy CPs. The values of the interband CP parameters (strength, threshold energy, broadening and phase angle) have been derived.

From the analysis of dielectric function the energies of the optical electron transitions at  $E_1$ ,  $E_1 + \Delta E_1$  and  $E_2$  CPs in the Brillouin zone have been identified and evaluated. The energy of  $E_1$ , which could be assigned to indirect band gap transitions, increases with crystallite size decrease. There is no measurable change in the energy of  $E_1 + \Delta E_1$ , which is probably related to the direct optical band-gap transitions. PL measurements were used to identify the electronic transitions inside the gap, as low intensity peaks observed in the sub-band gap energy region were difficult to evaluate from SE data. This study represents an attempt to resolve optical properties of anatase nanocrystals, related to interband transitions, as well as the electronic transitions mediated by defect

levels within the band gap.

## Acknowledgments

This work is supported by the Serbian Ministry of Science and Technological Development under project No. 141047.

## References

- [1] W.F. Zhang, M.S. Zhang, Z. Yin, Q. Chen, *Appl. Phys. B* **70**, 261 (2000).
- [2] P. Lautenschlager, S. Logothetidis, L. Vina, M. Cardona, *Phys. Rev. B* **32**, 3811 (1985).
- [3] K. Kumazaki, L. Vina, C. Umbach, M. Cardona, *Phys. Status Solidi B* **156**, 371 (1989).
- [4] B. Karunakaran, R.T. Rajendra Kumar, C. Viswanathan, D. Mangalraj, Sa.K. Narayandass, G. Mohan Rao, *Cryst. Res. Technol.* **38**, 773 (2003).
- [5] F. Curcio, M. Musci, N. Notaro, C. Nannetti, *Appl. Surf. Sci.* **36**, 52 (1989).
- [6] M. Šćepanović, Z.D. Dohčević-Mitrović, I. Hinić, M. Grujić-Brojčin, G. Stanišić, Z.V. Popović, *Mater. Sci. Forum* **494**, 265 (2005).
- [7] P. Petrik, *Phys. Status Solidi A* **205**, 732 (2008).
- [8] M. Grujić-Brojčin, M.J. Šćepanović, Z.D. Dohčević-Mitrović, I. Hinić, B. Matović, G. Stanišić, Z.V. Popović, *J. Phys. D, Appl. Phys.* **38**, 1415 (2005).
- [9] M. Leñn, S. Levchenko, A. Nateprov, A. Nicorici, J.M. Merino, R. Serna, E. Arushanov, *J. Phys. D, Appl. Phys.* **40**, 740 (2007).
- [10] P. Lautenschlager, M. Garriga, S. Logothetidis, M. Cardona, *Phys. Rev. B* **35**, 9174 (1987).
- [11] J.G. Albornoz, R. Serna, M. Leon, *J. Appl. Phys.* **97**, 103515 (2005).
- [12] D. Reyes-Coronado, G. Rodríguez-Gattorno, M.E. Espinosa-Pesqueira, C. Cab, R. de Coss, G. Oskam, *Nanotechnology* **19**, 145605 (2008).
- [13] P. Moriarty, *Rep. Prog. Phys.* **64**, 297 (2001).
- [14] K.M. Reddy, S.V. Manorama, A.R. Reddy, *Mater. Chem. Phys.* **78**, 239 (2003).
- [15] G. Guisbiers, O. Van Overschelde, M. Wautelet, *Appl. Phys. Lett.* **92**, 103121 (2008).
- [16] C. Ho, M.-C. Tsai, M.-S. Wong, *Appl. Phys. Lett.* **93**, 081904 (2008).
- [17] M.R. Teresa, M. Viseu, C. Isabel, *Vacuum* **52**, 115 (1999).
- [18] N. Daude, C. Gout, C. Jouanin, *Phys. Rev. B* **15**, 3229 (1977).
- [19] R. Asahi, Y. Taga, W. Mannstadt, A.J. Freeman, *Phys. Rev. B* **61**, 7459 (2000).
- [20] S. Kitazawa, S. Yamamoto, M. Asano, Y. Saitoh, S. Ishiyama, *Nucl. Instrum. Methods Phys. Res. B* **232**, 94 (2005).
- [21] H. Tang, H. Berger, P.E. Schmid, F. Levy, G. Burri, *Sol. State Commun.* **87**, 847 (1993).
- [22] S. Guha, K. Ghosh, J. G. Keeth, S.B. Ogale, S.R. Shinde, J.R. Simpson, H.D. Drew, T. Venkatesan, *Appl. Phys. Lett.* **83**, 3296 (2003).